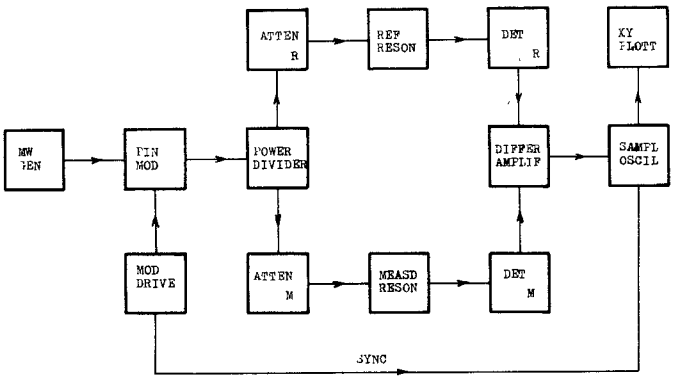

Fig. 1. Arrangement for the comparison decrement measuring of Q.

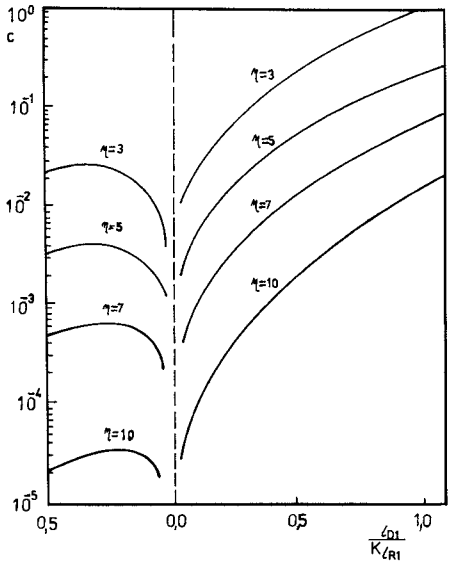

Fig. 2. Correction factor c as a function of $\iota_{D1}/(K\iota_{R1})$ Parameter $\eta = t_1\omega_{OR}/Q_{LR}$. For $\iota_{D1}/(K\iota_{R1}) < 0$, the correction factor is negative.

resulting error be eliminated using the corrected formula

$$Q_{LM} = Q_{LR}[1 + \iota_{D1}/(K\iota_{R1}) + c] \tag{9}$$

instead of (8). The index 1 is used to indicate integration over the finite interval $\langle 0, t_1 \rangle$ and c is the correction factor (see Fig. 2). The correction is negligible for large integration intervals

$$t_1 > 7Q_{LR}/\omega_{OR}$$

and small differences in resonators Q's

$$-0.5 < \iota_{D1}/(K\iota_{R1}) < +0.3.$$

If the integration interval is small

$$t_1 < 5Q_{LR}/\omega_{OR}$$

it is better to calculate Q_{LM} solving equation

$$Q_{LM}[1 - \exp(-\eta Q_{LR}/Q_{LM})] - Q_{LR}[1 + \iota_{D1}/(K\iota_{R1})][1 - \exp(-\eta)] = 0$$

where

$$\eta = t_1\omega_{OR}/Q_{LR}.$$

IV. Results

The described method was verified experimentally and the Q_L of three microwave-cavity X-band resonators was measured. The obtained results show a good reproducibility of better than 0.2 percent (see Table I), and high sensitivity of the comparison measuring set to change of Q_{LM}. The accuracy of measuring the value of Q_{LM} is limited by the accuracy of the reference resonator calibration, however, and is by no means as good as the reproducibility. The proposed method is advantageous even in such cases when a small change of Q is to be measured rather than its value.

TABLE I
Measured Values of Q of X-Band Cavity Resonators

Q_{LR} = 12 375 ±691†, η = 3

RDS No	$\frac{\iota_{D1}}{K\iota_{R1}}$	Q_{LM1}*	Q_{LM}**	Q_{LM}***
0161	0,20338 ±0,00211	14 892 ±26	15 592 ±36	15 202 ±397
0335	0,23640 ±0,00260	15 325 ±32	16 200 ±45	16 565 ±943
EX 3	-0,34972 ±0, 00112	6 047 ±14	7 709 ±13	7 849 ±348

* from equation /8/, assuming finite interval $\langle 0, t_1 \rangle$
** from eq. /10/
*** measured by the absolute decrement method
† standard deviation of Q_{LR} is not included in the Q_{LM1} and Q_{LM} deviations

References

[1] M. Sucher, "Measurement of Q," in *Handbook of Microwave Measurements*, vol. II, M. Sucher and J. Fox, Eds. New York: Polytechnic Press, 1963, ch VIII, pp. 478–490.

A 94-GHz Diode-Based Single Six-Port Reflectometer

HARRY M. CRONSON, SENIOR MEMBER, IEEE, AND ROBERT A. FONG-TOM, MEMBER, IEEE

***Abstract*—This paper describes design considerations and gives measurement results for a single six-port reflectometer constructed from WR-10 waveguide with silicon Schottky diode detectors. Tradeoffs between various types of power detectors are discussed along with criteria for six-port junction design. The merits of two calibration procedures are compared. Measurements at 94 GHz indicate good agreement between expected and experimental values of q-points and of a sliding mismatch with nominal 0.1 reflection coefficient.**

I. Introduction

Recently there has been a renewed interest in 94-GHz radar systems because of their combined advantages of small size, high resolution, and all weather visibility. If these systems are to satisfactorily progress from paper design to production, there must also be a parallel development of fast and accurate measurements. The natural trend has been to evolve millimeter-wave

Manuscript received December 31, 1981; revised April 13, 1982.
The authors are with the Sperry Research Center, Sudbury, MA 01776

0018-9480/82/0800-1260$00.75 ©1982 IEEE

measurement techniques from existing microwave methods. At present, however, there is no commercially available equipment to measure complex parameters at 94 GHz. This paper describes design considerations and gives amplitude and phase measurement results for a semi-automated 94-GHz single six-port reflectometer (SSPR). The capability to obtain complex reflection-coefficient information at these frequencies furnishes important development and testing procedures that have been proven so valuable in the microwave range.

Besides the work reported here, there appear to be several semi-automated systems under development. Oltman and Leach [1] have reported on the design of a 94-GHz system which uses mixers to beat down to a microwave ANA and has four-port junctions on either side of the device under test. At NBS, dielectric waveguide junctions have been used in both a single and dual six-port configuration [2]. A scalar transmission and reflection measurement test set has recently become commercially available [3].

The system described here is intended to satisfy the immediate need for a 94-GHz reflectometer with reasonable amplitude and phase accuracy. When first assembled, the main concern was to demonstrate that six-port measurements were feasible at 94 GHz with this waveguide system. Since then, it has undergone continuing stages of refinement as more is learned about systems characteristics. The system design is described in Section II, measurements in Section III, with conclusion in Section IV.

II. System Design

A. Hardware Description

A schematic diagram of the SSPR is shown in Fig. 1. The source, a 10-mW mechanically tunable Gunn oscillator, is followed by an isolator, coupler with harmonic mixer, single-pole double-throw mechanical switch, and the six-port junction with diode detectors. The six-port junction is made from discrete WR-10 waveguide components. The directional couplers designated by c_1, c_2, and c_3 have nominal 3-dB coupling value, whereas the 3-way divider couples about 5 dB to each of the sidearms and about 11 dB to the main arm. The alternate measurement port shown at the top uses the output of a high directivity 20-dB coupler for diode 1. The diode detectors are silicon Schottkys in a tunable mount (Hughes 47316-1100).

A photograph of the SSPR without the alternate measurement port is shown in Fig. 2. Not shown are the diode amplifiers, scanner (HP3495A), DVM (Fluke 8502A), and desk-top computer (HP9835A) needed to complete the analyzer.

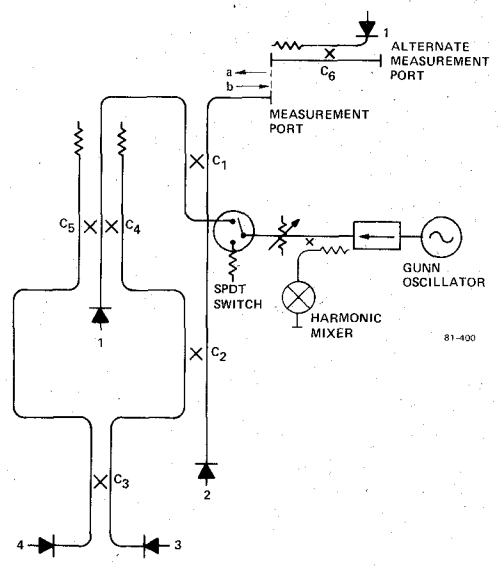

Fig. 1. Single six-port reflectometer schematic.

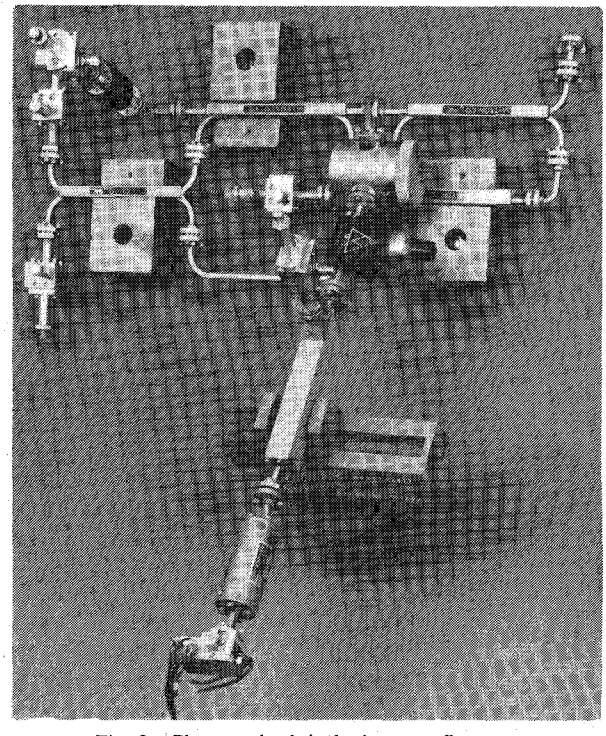

Fig. 2. Photograph of single six-port reflectometer.

B. Design Considerations

The above components were selected to satisfy requirements of simplicity, availability, and accuracy. The Gunn oscillator was used instead of an IMPATT source because the Gunn provides a relatively stable, low-noise output with enough power to operate the diode detectors at reasonable signal to noise ratios. The fact that the IMPATT can be electronically tuned over much larger frequency ranges was only of secondary importance for this application. Silicon Schottky diodes were chosen as power detectors over thermistors for several reasons. The most important is that they can operate effectively with much less power, thus avoiding expensive higher power sources. Another is that the associated amplifiers with the diodes are simpler and less expensive than thermistor bridge circuits. Although thermistors are more linear with power, the diodes are close enough to square law for this application when operated below -20 dBm. Point-contact diodes were also considered, but were abandoned because of low sensitivity. The SPDT switch was included to obtain diode offset voltage values with no incident power.

C. Six-Port Junction Design

The most important part of the system design was the six-port junction. Discrete waveguide components were chosen because of their availability, wide-band performance, and the possibility of fairly easy modifications. The particular arrangement of couplers shown in Fig. 1 was selected to meet three criteria. First, the incident and reflected signals at the detector ports should combine to give q-points that are fairly evenly distributed in the complex plane [4]. This insures that ill-conditioned situations will be avoided in the calculations. Secondly, the incident and reflected electrical path lengths to each detector port should be the same so the q-points are not frequency sensitive and result in specific ill-conditioned situations (see the Appendix). Lastly, as

many components as possible should be catalog items.

In the Appendix, it is shown that the calculated q-points for this six-port are

$$q_2 \cong j0.80$$
$$q_3 \cong -1.12 - j0.80$$
$$q_4 \cong 1.12 - j0.80.$$

III. Measurements

A. Calibration and Measurement Procedure

Two sets of reflection-coefficient measurements using different calibration procedures were made with the single six-port reflectometer at 94 GHz. The aim of the first set was to demonstrate that reasonable measurements were possible with this design. Therefore, a four standard calibration procedure [5], which could be quickly implemented, was used. It was later replaced with a more accurate NBS calibration procedure that required sliding terminations [6]. The same measurement routine was used in both cases.

The four standard procedure assumes that one of the ports (port 1 in this design) measures only the power incident on the device under test (DUT). This assumption simplifies the mathematics and permits the use of four standards instead of the usual seven [7]. For the six-port junction described here, this assumption was not satisfied by port 1, because part of the signal reflected from the measurement port reaches it via reflections from port 2. Thus, the alternate measurement port with the alternate port 1 had to be introduced to obtain reasonable results with the four standard procedure. Since coupler c_6 has about 40-dB directivity, the power incident to the alternate port 1 was very nearly equal to the incident power into the alternate measurement port. The four standards used were a matched load, quarter-wavelength offset short, and two known positions of a sliding short.

The NBS calibration procedure is based on a six-port to four-port reduction technique which requires one known standard, a sliding high-reflection mismatch, and a sliding low-reflection mismatch. One assumption is that the magnitude of the signal reflected from the sliding mismatch does not change with position. This appears to be well satisfied in practice. The one standard used in these experiments was a quarter-wavelength offset short.

B. Results

In the first set of measurements, the measured q-points were much different from their designed values because one arm of the junction was found to be 0.012 in shorter than the other. However, reasonable results were still possible as seen in Fig. 3. This is a plot in the complex reflection-coefficient (Γ) plane of the locus of a sliding mismatch, with $|\Gamma| \approx 0.1$, as it moves over one half-wavelength in roughly 30° steps. The circle is a least squares fit to the data points. The radius of the fitted circle is 0.10, and the magnitude of the offset is 0.02 (shown by the + sign). This offset is probably due to inaccuracies in the calibration procedure. The maximum difference between the data and the fit is 8%, and could be caused by temperature changes in the diodes between calibration and measurement or wobble in the sliding short track. This result accomplished the first goal of demonstrating the feasibility of the design.

Before taking a second set of measurements, the following improvements were made: the electrical length of the two arms was equalized using accurately machined spacers; the diodes and Gunn oscillator were temperature stabilized; the alternate measurement port was removed; and an isolator was added to port 2 to reduce reflections from this diode. It was found experimentally that this isolator improved the repeatability of the calibration. Using the NBS procedure, the q-points shown in Fig. 4 were obtained. These measured q-points agree reasonably well with calculated values and are fairly evenly distributed in the complex plane. The differences in the actual and designed values are due to nonideal couplers and reflections from the diode detectors. These differences do not affect the quality of the measurement as Fig. 5 demonstrates. This is a repeat of the measurement made in Fig. 3 with the improved system. As before, the circle drawn through the points is a least squares fit to the data. The radius of the fitted circle is 0.107, and the magnitude of the offset is 0.002. This offset, shown by the + sign, is probably due to misalign-

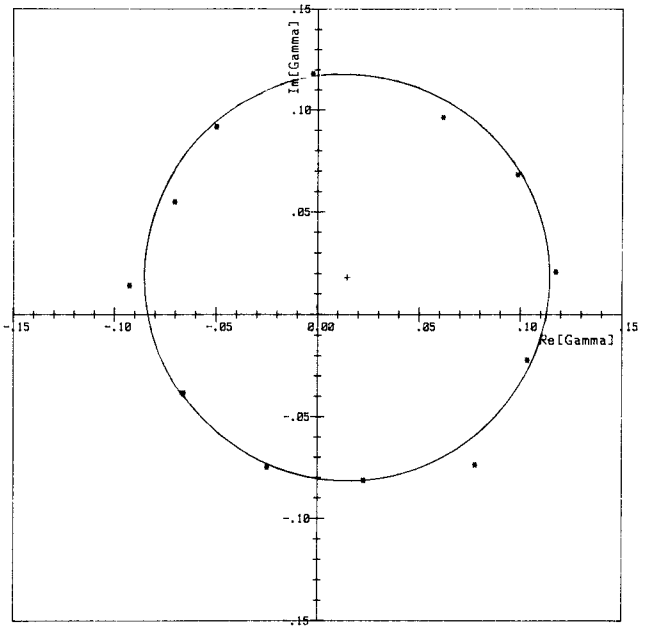

Fig. 3 Single six-port reflection-coefficient measurement using four standard calibration procedure. Nominal $|\Gamma| = 0.1$ sliding mismatch.

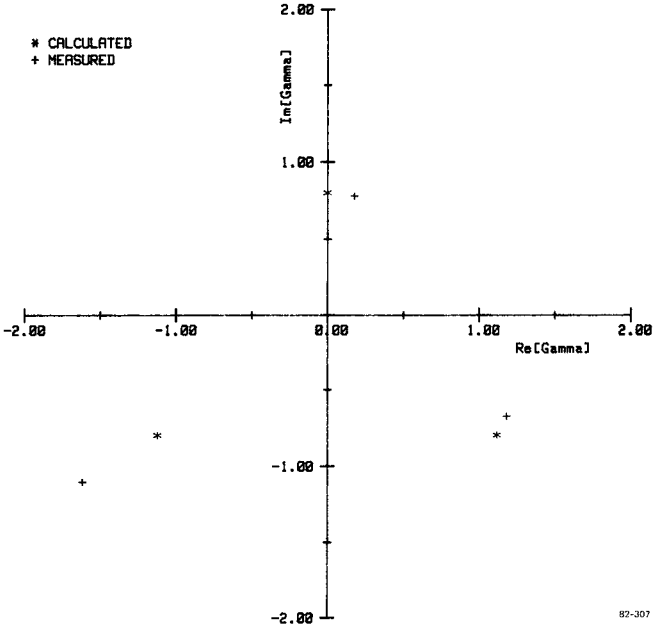

Fig. 4. Single six-port reflectometer calculated and measured q-points 94 GHz.

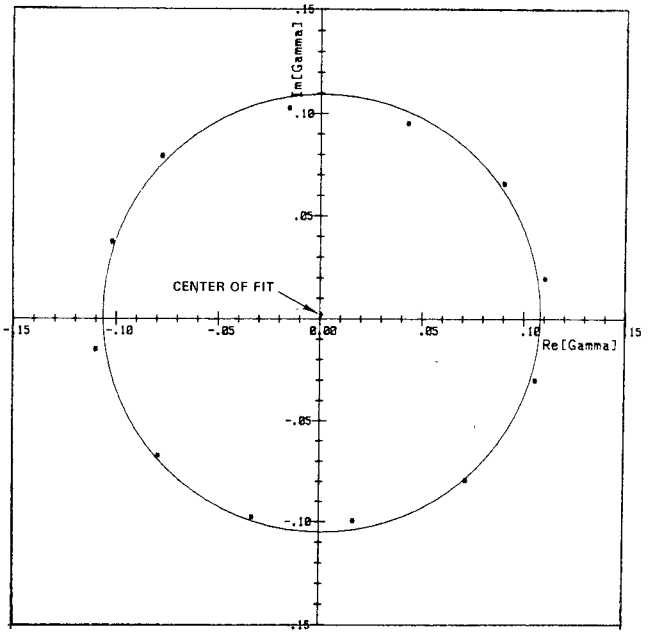

Fig. 5. Single six-port reflection coefficient measurement using NBS calibration procedure. Nominal $|\Gamma| = 0.1$ sliding mismatch.

ment of the flange, and slight differences in height between the waveguide under test and the sliding load waveguide used for calibration. The maximum difference in $|\Gamma|$ between the data and the fit is 5 percent, which can be explained by the wobble in the movement of the mismatch.

The stability of the system was measured by calibrating it each morning and making repeated measurements on a device of $|\Gamma| \approx 0.04$ during the course of the day without removing it from the test port. This was done for one week, storing the calibration constants on magnetic tape each day. At the end of the week the stored constants were recalled and used to measure the reflection coefficient of the same DUT without removing it from the test port. In this way, the stability of the junction over a period of one day and one week was measured without connect-disconnect errors affecting the results. The variations were ± 0.002 in the magnitude of Γ and $\pm 3°$ in the argument over a period of one day. The variations over one week, however, were ± 0.015 in the magnitude and $\pm 22°$ in the argument.

IV. Conclusions

We have demonstrated that a diode-based, *W*-band waveguide six-port junction can be built to within sufficient tolerance to achieve reasonable agreement with the design goals. With its present accuracy and good short-term stability, the system has proven useful for complex reflection coefficient measurements. Efforts are currently underway to upgrade the system by reducing error sources, improving long term stability by better temperature control, and extending the frequency range.

Appendix
Six-Port Junction *Q* Points

A. Definition

With reference to Fig. 1, the power at the detection ports P_i may be written as [4]

$$P_i = |A_i a + B_i b|^2, \qquad i = 1 \text{ to } 4 \tag{A-1}$$

where A_i, B_i are complex frequency dependent constants and a and b are the complex reflected and incident signals, respectively, at the measurement port, with the reflection coefficient Γ defined as

$$\Gamma = \frac{a}{b}. \tag{A-2}$$

Equation (A-1) can also be written as

$$P_i = |A_i b|^2 |\Gamma - q_i|^2 \tag{A-3}$$

where

$$q_i = -\frac{B_i}{A_i}. \tag{A-4}$$

These q_i are the q-points and, as (A-3) implies, P_i is proportional to the distances between Γ and q_i.

B. Frequency Dependence

If the junction is well known, the A_i and B_i may be determined analytically by tracing the paths of the reflected and incident signals from a common point, say the input of coupler c_1, to detector port i. Thus

$$A_i = C_{ai} e^{-(\alpha + j\beta) l_{ai}} \tag{A-5a}$$

$$B_i = C_{bi} e^{-(\alpha + j\beta) l_{bi}} \tag{A-5b}$$

where the C_{ai}, C_{bi} contain the relevant coupler transfer functions, α is the waveguide loss per unit length, β is the wave number, and l_{ai} and l_{bi} are the reflected and incident path lengths, respectively. Using (A-4) and (A-5)

$$q_i = -\frac{C_{bi}}{C_{ai}} e^{-(\alpha + j\beta)(l_{bi} - l_{ai})}. \tag{A-6}$$

In general, $l_{bi} - l_{ai} \neq 0$, and the q_i will rotate in the Γ plane as the frequency is changed. This frequency sensitivity should be avoided for two reasons. First, if the q_i are very frequency sensitive, one must be able to repeat the frequency very precisely between calibration and measurement for accurate measurements. Second, the frequency sensitivity means the q_i rotate in the Γ plane at different rates. If two pass close to each other, this will lead to an ill-conditioned situation with resulting poor measurement data.

The six-port junction described here was designed to have $l_{bi} - l_{ai} = 0$ for the configuration without the alternate measurement port. Dimensional measurements showed that a ~ 0.75-in piece of waveguide should be added to the measurement port to increase l_{ai}. Later, as a final adjustment, a 0.006-in shim was added on both ends of the line length connecting c_5 with c_3.

Even if $l_{bi} = l_{ai}$, some frequency dependence is found in practical junctions due to other factors. One is the frequency dependence of the couplers and bends in the system. Since these usually vary slowly with frequency, they play a minor role. Of more importance are reflections from ports other than the measurement port. Since the path lengths of these reflections are all different, they tend to contribute small random phase variations at the detector ports. This type of behavior is shown in experimentally measured q-points. Isolators or pads at the detectors can reduce this effect.

C. Determination by Analysis

As previously mentioned, the A_i, B_i, and therefore the q_i, can be found by tracing paths through the network. Using the transfer functions in Fig. 6, it can be shown, for example, that

$$c_{a2} = (1 - k_1^2)^{1/2} (1 - k_2^2)^{1/2} \tag{A-7a}$$

$$c_{b2} = -j(1 - k_1^2)^{1/2} k_2 k_4 / k_1. \tag{A-7b}$$

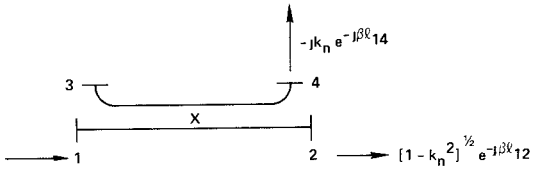

Fig. 6 Transfer function of ideal coupler C_n with k_n coupling coefficient

Using these equations, and noting that since $l_{bt}-l_{at}=0$ all the line length terms can be neglected, it can be shown that

$$q_2=\frac{jk_2k_4}{k_1\left(1-k_2^2\right)^{1/2}}. \tag{A-8a}$$

Similarly

$$q_3=-\frac{k_3k_5+jk_4\left(1-k_2^2\right)^{1/2}\left(1-k_3^2\right)^{1/2}}{k_1k_2\left(1-k_3^2\right)^{1/2}} \tag{A-9a}$$

$$q_4=\frac{k_5\left(1-k_3^2\right)^{1/2}-jk_3k_4\left(1-k_2^2\right)^{1/2}}{k_1k_2k_3}. \tag{A-10a}$$

From the design values

$$k_1=k_2=k_3=0.708$$

and

$$k_4=k_5=0.562.$$

Therefore

$$q_2=j0.80 \tag{A-8b}$$

$$q_3=-1.12-j0.80 \tag{A-9b}$$

$$q_4=1.12-j0.80. \tag{A-10b}$$

Fig. 4 shows that the measured q-points were fairly close to these values.

ACKNOWLEDGMENT

The authors wish to acknowledge many helpful discussions with L. Susman of Sperry Research Center. The six-port junction could not have been constructed without the expertise and generous cooperation of T. Kozul of Baytron Co., Inc. T. Kirkland of SRC provided diligent assistance in performing the experiments. We would also like to thank M. Weidman of NBS for supplying the NBS Calibration Program.

REFERENCES

[1] H. G. Oltman and H. A Leach, "A dual four-port for automatic network analysis," in *1981 IEEE MTT-S Internat. Symp. Dig.*, pp 69–72
[2] M. Weidman, Panel Session, "Millimeter wave automatic network analyzers," presented at 17th ARFTG Workshop, (Los Angeles, CA), June 18, 1981.
[3] Product Feature, Millimeter-wave network analyzer offers computer control, MSN, July 1981, p 98.
[4] G F. Engen, "The six-port reflectometer: An alternative network analyzer," *IEEE Trans Microwave Theory Tech.*, vol MTT-25, pp. 1075–1080, Dec 1977.
[5] H M Cronson and L. Susman, "A New calibration technique for automated broadband microwave measurements," in *Proc. 6th Euro. Microwave Conf.*, (Rome, Italy) Sept. 1976, p. 205.
[6] G. F. Engen, "Calibrating the six-port reflectometer by means of sliding terminations," *IEEE Trans. Microwave Theory Tech.*, vol. MTT-26, pp. 951–957, Dec. 1978.
[7] D Woods, "Analysis and calibration theory of the general six-port reflectometer employing four amplitude detectors," in *Proc. Inst. Elec. Eng.*, vol 126, Feb. 1979, pp. 221–228.

Analysis of the Shielded-Strip Transmission Line with an Anisotropic Medium

HISASHI SHIBATA, SHINYA MINAKAWA, AND RYUITI TERAKADO

***Abstract*—Analysis of the shielded stripline with an anisotropic medium is presented by means of an affine transformation and a conformal mapping technique. The capacitance is represented in the function $K'(k)/K(k)$ with a modified modulus k, which is obtained by multiplying d, the width between the ground planes in [1, table I], by α. The parameter α relates to the anisotropic medium. The exact distributions of equipotentials and lines of electric flux in the anisotropic medium are also presented.**

I. INTRODUCTION

A structure with homogenous isotropic medium in which the conductor is a strip of zero thickness located on the center inside two parallel infinite grounded planes has been exactly analyzed [1]–[7] by using a conformal mapping technique.

The object of this paper is to propose analytical formulas for the capacitance and field distributions of the structure with an anisotropic medium shown in Fig. 1(a). An affine transformation which was reported by Kusase and Terakado [8] is used to implement the present work. Application of the transformation leads us to analysis of the structure with a corresponding isotropic medium as shown in Fig. 1(b), and a conformal mapping technique is applied to the structure with the isotropic medium. Thus, the capacitance of the structure of Fig. 1(a) is represented in the function of complete elliptic integrals of the first kind, even though the stripline is composed of the anisotropic medium. The modulus which determines the elliptic integrals is merely obtained by multiplying d, the width between the ground planes in [1, table 1], by α. The parameter α is determined by the principal axes-relative dielectric constants of the anisotropic medium and the angle between the principal axes and the ground plane. In addition, we present an expansion for the capacitance in the series of $\exp(-b\pi/\alpha h)$, where b and h are dimensions of the structure. In Section III, we present the exact distributions of equipotentials and lines of electric flux in the structure shown in Fig. 1(a). The distributions will show that equipotential and flux lines do not perpendicularly intersect each other.

II. AFFINE AND CONFORMAL TRANSFORMATIONS

Now consider the structure shown in Fig. 1(a). The two-dimensional space between two parallel infinite grounded planes is assumed to be filled with the anisotropic medium of the following permittivity tensor:

$$\bar{\epsilon}=\epsilon_0\begin{pmatrix}\epsilon_{\parallel} & 0\\ 0 & \epsilon_{\perp}\end{pmatrix} \tag{1}$$

where $\epsilon_{\parallel}$, $\epsilon_{\perp}$, and ϵ_0 are the principal axes-relative dielectric constants of the anisotropic medium and the permittivity of vacuum, respectively. The tensor for the $x-y$ coordinates is obtained by rotating the principal axes with the angle θ as shown in

Manuscript received November 5, 1981; revised March 3, 1982.

H Shibata and S. Minakawa are with the Department of Electrical Engineering, Ibaraki Technical College, Katsuta, Ibaraki, 312, Japan.
R. Terakado is with the Department of Electrical Engineering, Faculty of Engineering, Ibaraki University, Hitachi, Ibaraki, 316, Japan

0018-9480/82/0800-1264$00.75 ©1982 IEEE